Published in final edited form as:

Biochem Biophys Res Commun. 2018 January 01; 495(1): 526–532. doi:10.1016/j.bbrc.2017.10.170.

Surfactant protein D attenuates nitric oxide-stimulated apoptosis in rat chondrocyte by suppressing p38 MAPK signaling

Yan Zhou[a], **Jianghua Ming**[a], **Yaming Li**[a], **Xianjin Du**[a], **Ming Deng**[a], **Bin He**[a], **Jianlin Zhou**[a], **Guirong Wang**[b,**], and **Shiqing Liu**[a]

[a]Department of Orthopedics, Central Laboratory, Renmin Hospital of Wuhan University, Wuhan 430060, China

[b]Department of Surgery, SUNY Upstate Medical University, Syracuse, NY 13210, USA

Abstract

Innate immune molecule surfactant protein D (SP-D), a member of the C-type lectin protein family, plays an indispensable role in host defense and the regulation of inflammation in the lung and other tissues. Osteoarthritis (OA) is a degenerative disease of cartilage, with inflammation that causes pathologic changes and tissue damage. However, it is unknown whether there exist SP-D expression and its potential role in the pathogenesis of OA. In this study, we examined SP-D expression and explored its biological function in a sodium nitroprusside (SNP)-stimulated rat chondrocytes and surgically-induced rat OA model. We found SP-D expression in both human and rat articular chondrocytes, with higher level in normal chondrocytes compared to in OA chondrocytes. Furthermore, *In vivo* study demonstrated that recombinant human SP-D (rhSP-D) ameliorated cartilage degeneration in surgically-induced rat OA model. *In vitro* cell culture study showed that rhSP-D markedly inhibited the expression of caspase-3 as an apoptosis biomarker, and decreased phosphorylation of p38 mitogen-activated protein kinase (MAPK), which resulted in maintaining normal nuclear morphology and increasing mitochondrial membrane potential in SNP-stimulated rat chondrocytes. Collectively, these findings indicate that SP-D expresses in articular chondrocytes and suppresses SNP-stimulated chondrocyte apoptosis and ameliorates cartilage degeneration via suppressing p38 MAPK activity.

Keywords

Surfactant protein D; Osteoarthritis; Chondrocyte; Sodium nitroprusside; Apoptosis

1. Introduction

Osteoarthritis (OA) is a prevalent arthritic disease characterized by progressive breakdown of cartilage tissue, remodeling of subchondral bone, osteophyte formation, and synovial

Correspondence to: Shiqing Liu.

**Corresponding author. Department of Surgery, SUNY Upstate Medical University, 750 E. Adams St., Syracuse, NY 13210, USA. Wangg@upstate.edu (G. Wang).

Conflicts of interest

The authors confirm no competing interests.

inflammation, which has considerable influences on the quality of an individual's life, especially in this aging society [1]. Common clinical symptoms of OA include joint pain, joint dysfunction and malformation, and the pathological process involves multifactorial disorders in which apoptosis and chronic inflammation in articular cartilage chondrocyte have critical roles [2]. Enhanced chondrocyte apoptosis is generally indicated to be a marker of cartilage degeneration in aggravation [3]. The chronic, low-grade inflammation, due to the interplay between the innate immune system and elements including mechanical damage and metabolic dysfunction, contributes to joint degeneration in OA [4]. The potential of therapeutic strategies against low-grade inflammation and chondrocyte apoptosis at early stage of OA can alter the course of the disease.

Surfactant protein D (SP-D), a member of the C-type lectin protein family, plays a crucial role in host defense and regulating inflammation in the lung and other tissues, where SP-D is substantially expressed and located in the respiratory epithelium [5]. The structure of SP-D is comprised of four domains, including N-terminus cysteine-rich domain, triple-helical collagen-like domain, neck region and carbohydrate recognition domain (CRD) [6]. Extrapulmonary tissues/organs SP-D expression has been recognized, such as kidney [7], digestive tract and mesentery [8], nasal epithelium [9], salivary glands and saliva [10], pancreas [11], and prostate and reproductive system [12]. Furthermore, SP-D is expressed in the synovial fluid to vary degrees in rheumatoid arthritis (RA), which reveals a characteristic aspect in the pathogenesis of RA as in lung [13,14]. Nevertheless, no relevant report is available on SP-D expression and biological functions in the pathogenesis of OA. As an important immune molecule, SP-D plays a vital role in modulating inflammatory responses and inhibiting apoptosis, it is reasonable to speculate that SP-D is expressed in articular cartilage and make contribution to the innate immune mechanism in the pathogenesis of OA. In the current study, we identified SP-D expression in articular cartilage and chondrocytes, and examined the role of SP-D on chondrocyte apoptosis and cartilage degeneration, and then elucidated the underlying molecular mechanisms.

2. Materials and methods

2.1. Materials

The p38 MAPK inhibitor SB203580 and rabbit antibodies against caspase-3 were obtained from Calbiochem (San Diego, CA, USA). Glyceraldehyde-3-phosphate dehydrogenase (GAPDH), phosphop38 MAPK (p-p38 MAPK), and p38 MAPK antibodies were obtained from Abcam (Cambridge, UK). Recombinant human SP-D (rhSP-D) (CSB-YP021175HU) was purchased from Huamei Biotech Co., Ltd (Wuhan, Hubei, China).

2.2. Histological analysis

Human OA cartilage was obtained from patients undertaking total knee arthroplasty. Normal tissue samples used as control were obtained from patients undergoing post-traumatic amputation with no history of OA. The patient's agreement as well as approval of the local ethics committee were acquired prior to harvesting tissue samples. The cartilage specimens were fixed in 4% paraformaldehyde, decalcified three weeks in Calci-Clear slow solution [10% (w/v) EDTA, pH 7.4], and then embedded in paraffin wax. Hematoxylin and Eosin

(H&E) staining and toluidine blue-O staining were executed on 5 mm serial sagittal sections of cartilage.

2.3. Immunohistochemical analysis

An immunohistochemical study of human and rat joint tissues were performed according to the manufacturer's instructions. The rat articular cartilage and synovial tissues were obtained from our previous research [15]. The isolated knee joints were processed for immunohistochemistry. The serial sagittal sections of cartilage and synovial tissues were incubated overnight at 4 °C with primary antibody against SP-D (1:400 dilution; Santa Cruz Biotechnology, CA, USA). The immunohistochemical reaction was visualized by diaminobenzidine (Boster Biological Engineering, Wuhan, China), and then counterstained with haematoxylin. The images were captured under an Olympus microscope (Olympus Corporation, Tokyo, Japan) with × 200 and × 400 magnification. Five representative sections of each joint in randomly selected high power field (× 400 magnification) were evaluated on slides. The integrated optical density (IOD) was calculated using Image-Pro Plus 6.0 image analysis software (Media Cybernetics Co., USA).

2.4. Establishment of a rat OA model

Twenty-five male SD rats (200–250 g body weight) purchased from the Center for Animal Experiment/ABSL-III Laboratory of Wuhan University were used for this study. The rats were assigned randomly into five groups including sham-operated, rhSP-D (High-dose), OA-induction, OA + rhSP-D (Low-dose), and OA rhSP-D (High-dose) groups, and anaesthetized intraperitoneallyþwith trichloroacetaldehyde hydrate (300 mg/kg) in sterile saline. The anterior cruciate ligament transection together with medial menisci resection (ACLT + MMx) in the right knee joint was carried out to establish the rat OA model according to previous research[16]. For the sham-operated and rhSP-D (High-dose) groups, the wounds were sutured after exposing the knee joint cartilage surface. The rats were located in an electric rotating cage for 30 min per day to stimulate OA model from the first week after surgery as we previously described [17]. H&E staining showed that rat OA model was established by exercise in the electric rotating cage at the fourth week after surgery [15]. Four weeks after the surgery, the rats knee joints in OA + rhSP-D (Low-dose), OA + rhSP-D (High-dose) and rhSP-D (High-dose) groups were injected intraarticularly with 30 μl of 20 and 40 μg/mL rhSP-D. Meanwhile, the rats in sham-operated and OA-induction groups received an injection of 30 μl PBS. The rats were sacrificed by cardiac exsanguinations at the 10th week after surgery. H&E staining was performed on serial sagittal slices of rat knee articular cartilage. Semi-quantitative histopathological grading was completed according to a modified Mankin scoring system [18]. All procedures were approved by the Animal Care and Use Committee of Medical School, Wuhan University.

2.5. Cell culture

Primary chondrocytes were isolated from the knee joints of 5-day-old Sprague-Dawley (SD) rats purchased from the Center for Animal Experiment/ABSL-III Laboratory of Wuhan University, Wuhan, China, and processed by trypsin and collagenase. The isolated cells cultured in Dulbecco's modified Eagle's medium (DMEM)/F12 (Hyclone, USA) complete culture medium (containing 10% fetal bovine serum and 100 units/ml of penicillin and

streptomycin) at 37 °C and 5% CO_2. All protocols were permitted by the Institutional Ethics Committee of Medical School, Wuhan University.

2.6. Cell viability assay

Cell counting kit-8 (CCK-8; Dojindo Laboratories, Kumamoto, Japan) was employed to evaluate chondrocyte viability according to the manufacturer's protocol. The third passage chondrocytes were plated in 96-well plates (0.5×10^4/well) for 24 h, and then treated with different concentrations of rhSP-D (0, 2.5, 5, 10, and 20 μg/mL) for 12 and 24 h. 100 μl of 10% CCK-8 solution was added to each well and incubated for 1–4 h. Then the optical density value was read by ELISA reader (Bio-Tek, Model EXL800, USA) at 450 nm. Cell viability was determined as percentage of the control group.

2.7. Western bloting analysis

Proteins in cultured chondrocytes were isolated using a total protein extraction kit according to the manufacturer's instructions. The extracted cellular proteins were loaded on a sodium dodecyl sulfate-polyacrylamide gel electrophoresis (SDS-PAGE). The proteins were transferred to polyvinylidene difluoride (PVDF) membranes. The PVDF membranes were cut into several strips according to the protein marker size and appropriate membrane strip was incubated overnight at 4 °C with primary antibodies against caspase-3, p-p38 MAPK, p38 MAPK, and GAPDH, respectively. The blots were then incubated with the respective peroxidaseconjugated secondary antibodies for 1 h. Chemiluminescent signals were imagined with enhanced chemiluminescence Western blot detection reagent (Amersham Biosciences, Piscataway, NJ, USA). Immunoblot bands were analyzed using Odyssey infrared imaging system (LI-COR, NE, USA).

2.8. Apoptosis analysis by Hoechst 33342 nuclear staining

The adherent chondrocytes were exposed to different concentrations of rhSP-D for 2 h before 0.75 mM SNP (Youcare Pharmaceutical Group Co., Ltd, Beijing, China) co-treatment for 24 h. The cells were fixed with 4% (v/v) paraformaldehyde for 30 min, and permeabilized with 1 mL Hoechst 33342 dye (5 μg/mL, Beyotime Institute of Biotechnology, Haimen, China) for 20 min. After washing with PBS, the cells were observed under an Olympus microscope. Each assay was achieved in quadruple and repeated three times. The apoptotic cell proportion was measured by percentage of the chondrocytes with nucleic morphological changes to the total cells of three random visual fields.

2.9. Mitochondrial membrane potential analysis by Rhodamine-123 staining

Mitochondrial membrane potential was assessed according to the uptaking capacity of chondrocytes to the Rhodamine-123 fluorescent dye (Sigma-Aldrich, St. Louis, MO, USA). The adherent chondrocytes were exposed to different concentrations of rhSP-D for 2 h before 0.75 mM SNP co-treatment for 24 h. 2 mL of DMEM/F12 complete culture medium with 10 mM Rhodamine-123 was added to each well and incubated for 30 min at 37 °C. After washing with PBS, the positive chondrocytes stained with green fluorescence were observed under an Olympus microscope. The cellular fluorescence values were measured using Image-Pro Plus 6.0 software.

2.10. Immunofluorescence assay

Adherent chondrocytes at 70% confluency were grown on glass coverslips in 6-well plates and starved for 12 h before treatment. After fixation with 4% paraformaldehyde for 20 min, chondrocytes were permeabilized with 0.5% Triton X-100 buffer (Beyotime, Jiangsu, China) for 5 min, and then blocked with 1% bovine serum albumin at 4 °C for 10 min. Chondrocytes were cultured with SP-D antibody (1:400 dilution) for 2 h followed by incubated with Cy3-labeled secondary antibody (1:100 dilution; Boster Biological Engineering, Wuhan, China) in the dark for 1 h. Nuclei were counter-stained with DAPI (KeyGEN Biotech, Nanjing, China) for 10 min. Slides were visualized by an Olympus microscope, and the IOD of SP-D was calculated by Image-Pro Plus 6.0 image analysis software.

2.11. Statistical analysis

Data were presented as mean ± standard error of the mean (S.E.M). Statistical difference were compared using One-way analysis of variance (ANOVA) and Student's t-test with SPSS 16.0 software. $P < 0.05$ is considered statistically significant. The statistical tests were completed using GraphPad Prism software, version 5.0 (San Diego, CA, USA).

3. Results

3.1. The expression of SP-D and changes of its level in human and rat joint tissues

To examine SP-D role in human knee cartilage, we compared SPD expression and the change of its level by immunohistochemical analysis in human normal and OA cartilage obtained from subjects undertaking total knee arthroplasty, as well as normal cartilage samples from post-traumatic amputation subjects, which were confirmed by histopathological analysis (Fig. 1A). Immunohistochemical analyses revealed that the level of total SP-D expression in normal cartilage was higher than in OA cartilage of human (***$p < 0.001$, Fig. 1A). Meanwhile, we investigated SP-D expression of the sham-operated and OA-induction rat knee cartilage and synovial tissue. As shown in Fig. 1B and C, the SP-D level in the sham-operated group was significantly higher than that of OA-induction group in both rat cartilage and synovial tissue (**$p < 0.01$ and ***$p < 0.001$). These data indicate that the decline of SP-D expression is a characteristic event during human and rat OA development.

3.2. Effects of rhSP-D on histopathology in rat OA cartilage

Histopathological changes were conducted on rat cartilage surface and matrix layer (Fig. 2A). In the sham-operated and rhSP-D (High-dose) groups, regular morphological structure was observed in articular cartilage, while the cartilage surface was uneven in the OA-induction group. With the injection of rhSP-D (20 and 40 μg/mL), the thickness of rat knee articular cartilage improved considerably, and the cartilage erosion was essentially ameliorated in a dosage-dependent manner. According to the modified Mankin scores (Fig. 2B), the severity of cartilage degradation in OA + rhSP-D (20 and 40 μg/mL) groups was lower than that of the OA-induction group ($^{\#}p < 0.05$ and $^{\#\#}p < 0.01$). These findings

suggest that rhSPD is able to ameliorate cartilage degeneration in surgically-induced rat OA model.

3.3. Effect of rhSP-D on chondrocyte viability

The viability effect of rhSP-D on chondrocytes was estimated by CCK-8 assay with different concentrations for 12 and 24 h (Fig. 3A). The results displayed that rhSP-D at concentrations ranging from 5 to 20 mg/mL had no cytotoxic effect on rat chondrocytes.

3.4. rhSP-D decreased caspase-3 and p-p38 MAPK activation in SNP-stimulated chondrocytes

To explore the potential mechanism of rhSP-D decreasing chondrocyte apoptosis, the protein expression of cleaved caspase-3 was determined. As shown in Fig. 3B, compared with the control group, the expression of cleaved caspase-3 increased significantly in SNP-stimulated rat chondrocytes, and with dose-dependent manner after exposure to rhSP-D protein from 5 to 10 μg/mL. Similarly, The total and phosphorylation level of p38 MAPK in different groups were evaluated. As shown in Fig. 3C, the expression of p-p38 MAPK in 0.75 mM SNP-stimulated chondrocytes was higher than that in the control group, while pretreatment with rhSP-D (10 μg/mL) blocked the SNP-stimulated up-regulation of pp38 MAPK. The p38 MAPK inhibitor SB203580 (10 μM) significantly decreased the p-p38 MAPK expression compared with the rhSP-D-mediated regulation. The level of p38 MAPK in different groups presented no apparent changes. These results indicate that rhSP-D possesses anti-apoptotic function and suppresses p38 MAPK activation in SNP-stimulated chondrocytes.

3.5. Effect of rhSP-D on nucleic morphology in SNP-stimulated chondrocytes

We examined the changes of chondrocyte nucleic morphology by Hoechst 33342 nuclear staining. As shown in Fig. 4A, chondrocyte nuclei were round and stained evenly in the control group. In the SNP group, about 46% of the cells appeared with condensed and fragmented nuclei. The proportion of chondrocyte nuclei condensation and fragmentation reduced significantly after the treatment of 10 μg/mL rhSP-D compared with the SNP group ($^{\#\#}p < 0.01$). These data suggest that rhSP-D attenuates nucleic morphological changes in SNP-stimulated rat chondrocytes.

3.6. Effect of rhSP-D on mitochondrial membrane potential in SNP-stimulated chondrocytes

The changes of mitochondrial membrane potential were examined by Rhodamine-123 staining. As shown in Fig. 4A, the mitochondrial membrane potential in the SNP group showed a significant reduction as compared to the control group (***$p < 0.001$), which could be significantly inhibited by the treatment of 10 mg/mL rhSP-D ($^{\#}p < 0.05$). These indicate that rhSP-D increases mitochondrial membrane potential in SNP-stimulated rat chondrocytes.

3.7. Immunoflourescence staining of SP-D expression in rat chondrocytes

As shown in Fig. 4B, immunoflourescence staining was performed to detect SP-D expression in chondrocytes. The mean density of SP-D expression was significantly high in the control group, which could be considerably inhibited by the stimulation of0.75 mM SNP (***$p < 0.001$). After the treatment of 10 μg/mL rhSPD, the expression level of SP-D significantly increased than the SNP group ($^{\#\#}p < 0.01$). These demonstrate that rhSP-D can stimulate SP-D expression in SNP-stimulated rat chondrocytes.

4. Discussion

In this study, we have demonstrated the expression and activity of SP-D on cartilage and synovial tissue of human and rat. By *in vitro* and *in vivo* approaches, we examined the effects of rhSP-D on SNP-stimulated rat chondrocyte apoptosis, as well as on articular cartilage in a surgically-induced rat OA model. Our data suggested that rhSP-D attenuated chondrocyte apoptosis and protected articular cartilage from degeneration in rat OA model possibly through suppressing p38 MAPK activity. Thus, SP-D plays a significant role in modulation of apoptosis in chondrocytes.

The role of innate immune system has been verified in OA pathogenesis, and activation of the innate immune system is essentially involved in initiation of low-grade inflammation, synovitis development, cartilage degeneration, and susceptibility to OA disease [19]. The damage of cellular and cartilage extracellular matrix breakdown products from injury, microtrauma, or normal aging degeneration causes damage-associated molecular patterns (DAMP) that motivate the innate immune system [20]. DAMP prompts a sterile inflammatory response through interaction with particle recognition receptors (PRRs), such as Toll-like receptors (TLRs) on the membrane of immune cells [21]. Sustained or dys-regulated activation of PRR-DAMP-stimulated inflammation can be destructive in OA [19]. As a kind of PRRs, SP-D has been found to contribute remarkably to surfactant homeostasis and innate host defense, and to exhibit specific binding to the extracellular domains of recombinant TLR4 through its CRD [22]. SP-D can inhibit TLR4 expression and inflammatory cytokines in human corneal epithelial cells through TLR4 signaling pathway during fungal infection [23]. SP-D can inhibit cell apoptosis and modulating NF-κB-mediated inflammation in sepsis-stimulated acute pancreatic injury [11]. The present study is the first to suggest that SP-D expression was observed in chondrocyte, and explain the critical role in modulation of SP-D in OA progression.

With the consequence of chondrocytes apoptosis, articular homeostasis is compromised, which results in the destruction of cartilage and further accelerates pathological changes in OA, including gradually decreased chondrocytes, cartilage degeneration, and osteophyte formation [24]. Weakening the apoptotic process may ameliorate the development of cartilage degeneration. In this study, fresh SNP in 0.75 mM concentration was used to stimulate chondrocyte apoptosis as our previous research [17]. Our *in vitro* results suggested that SP-D exerted an inhibitory effect on SNP-stimulated apoptosis in chondrocytes, and down-regulated the protein expression of activated caspase-3. The *in vivo* study showed that the Mankin scores were considerably lower and thicker cartilage layer were perceived in the OA + rhSP-D-injected groups as to the OA-induction group. Therefore, SP-D expression in

chondrocyte and the inhibitory effect of SP-D on chondrocyte apoptosis by SNP stimulation has a prospection to enhance our understanding of the OA pathogenesis and explore the potential of therapeutic strategies that target this protein in prevention and treatment of OA.

Activation of p38 MAPK has participated in chondrocyte apoptosis. Conversely, inhibition of p38 MAPK has been shown the protective effect on cartilage degeneration in animal OA model. It has been found by Gardai et al. [25] that in the absence of microbial ligands and cell debris, binding of SP-D to macrophages by the CRD region was proposed to be anti-inflammatory by blocking p38 MAPK signaling. In the present study, SP-D attenuated SNP-stimulated chondrocyte apoptosis via suppressing p38 MAPK activity. Taken together from previous and current findings, the chondroprotective effect of SP-D may be ascribed to the p38 MAPK-mediated anti-apoptotic effect in SNP-stimulated rat chondrocytes.

In conclusion, this study has revealed that SP-D is expressed in chondrocyte and joint articular cartilage, and exerts inhibitory effect in chondrocyte apoptosis, which may hinder OA progress. Further studies of SP-D interacting with transmembrane receptors are required to validate these mechanisms.

Funding

This work was supported by the Fundamental Research Funds for the Central Universities (Grant no, 2042017kf0139), the National Natural Science Foundation of China (Grant no. 81601670), and NIH/R01HL136706

References

[1]. Thysen S, Luyten FP, Lories RJ, Targets, models and challenges in osteoarthritis research, Dis. Model Mech 8 (2015) 17–30. [PubMed: 25561745]

[2]. Cong L, Zhu Y, Tu G, A bioinformatic analysis of microRNAs role in osteo-arthritis, Osteoarthr. Cartil 25 (2017) 1362–1371. [PubMed: 28336453]

[3]. Hosseinzadeh A, Kamrava SK, Joghataei MT, Darabi R, Shakeri-Zadeh A,Shahriari M, Reiter RJ, Ghaznavi H, Mehrzadi S, Apoptosis signaling pathways in osteoarthritis and possible protective role of melatonin, J. Pineal Res 61 (2016) 411–425. [PubMed: 27555371]

[4]. Zhuo Q, Yang W, Chen J, Wang Y, Metabolic syndrome meets osteoarthritis, Nat. Rev. Rheumatol 8 (2012) 729–737. [PubMed: 22907293]

[5]. Wright JR, Immunoregulatory functions of surfactant proteins, Nat. Rev. Immunol 5 (2005) 58–68. [PubMed: 15630429]

[6]. Reinhardt A, Wehle M, Geissner A, Crouch EC, Kang Y, Yang Y, Anish C, Santer M, Seeberger PH, Structure binding relationship of human surfactant protein D and various lipopolysaccharide inner core structures, J. Struct. Biol 195 (2016) 387–395. [PubMed: 27350640]

[7]. Liu J, Abdel-Razek O, Liu Z, Hu F, Zhou Q, Cooney RN, Wang G, Role of surfactant proteins A and D in sepsis-induced acute kidney injury, Shock 43 (2015) 31–38. [PubMed: 25255378]

[8]. Bourbon JR, Chailley-Heu B, Surfactant proteins in the digestive tract, mesentery, and other organs: evolutionary significance, Comp. Biochem. Physiol. A Mol. Integr. Physiol 129 (2001) 151–161. [PubMed: 11369540]

[9]. Kim JK, Kim SS, Rha KW, Kim CH, Cho JH, Lee CH, Lee JG, Yoon JH, Expression and localization of surfactant proteins in human nasal epithelium, Am. J. Physiol. Lung Cell Mol. Physiol 292 (2007) L879–L884. [PubMed: 17209137]

[10]. Brauer L, Moschter S, Beileke S, Jager K, Garreis F, Paulsen FP, Human parotid and submandibular glands express and secrete surfactant proteins A, B, C and D, Histochem Cell Biol 132 (2009) 331–338. [PubMed: 19484255]

[11]. Liu Z, Shi Q, Liu J, Abdel-Razek O, Xu Y, Cooney RN, Wang G, Innate immune molecule surfactant protein D attenuates sepsis-induced acute pancreatic injury through modulating apoptosis and NF-kappaB-mediated inflammation, Sci. Rep 5 (2015) 17798. [PubMed: 26634656]

[12]. Oberley RE, Goss KL, Dahmoush L, Ault KA, Crouch EC, Snyder JM, A role for surfactant protein D in innate immunity of the human prostate, Prostate 65 (2005) 241–251. [PubMed: 15948134]

[13]. Kankavi O, Increased expression of surfactant protein A and D in rheumatoid arthritic synovial fluid (RASF), Croat. Med. J 47 (2006) 155–161. [PubMed: 16489709]

[14]. Christensen AF, Sorensen GL, Horslev-Petersen K, Holmskov U, Lindegaard HM, Junker K, Hetland ML, Stengaard-Pedersen K, Jacobsen S,Lottenburger T, Ellingsen T, Andersen LS, Hansen I, Skjodt H, Pedersen JK, Lauridsen UB, Svendsen A, Tarp U, Podenphant J, Vestergaard A, Jurik AG,Ostergaard M, Junker P, Circulating surfactant protein -D is low and correlates negatively with systemic inflammation in early, untreated rheumatoid arthritis, Arthritis Res. Ther 12 (2010). R39. [PubMed: 20211020]

[15]. Zhou Y, Liu SQ, Peng H, Yu L, He B, Zhao Q, In vivo anti-apoptosis activity of novel berberine-loaded chitosan nanoparticles effectively ameliorates osteoarthritis, Int. Immunopharmacol 28 (2015) 34–43. [PubMed: 26002585]

[16]. Hayami T, Pickarski M, Zhuo Y, Wesolowski GA, Rodan GA, Duong LT, Characterization of articular cartilage and subchondral bone changes in the rat anterior cruciate ligament transection and meniscectomized models of osteoarthritis, Bone 38 (2006) 234–243. [PubMed: 16185945]

[17]. Zhou Y, Liu SQ, Yu L, He B, Wu SH, Zhao Q, Xia SQ, Mei HJ, Berberine prevents nitric oxide-induced rat chondrocyte apoptosis and cartilage degeneration in a rat osteoarthritis model via AMPK and p38 MAPK signaling, Apoptosis 20 (2015) 1187–1199. [PubMed: 26184498]

[18]. Wang CJ, Huang CY, Hsu SL, Chen JH, Cheng JH, Extracorporeal shock-wave therapy in osteoporotic osteoarthritis of the knee in rats: an experiment in animals, Arthritis Res. Ther 16 (2014). R139. [PubMed: 24994452]

[19]. Robinson WH, Lepus CM, Wang Q, Raghu H, Mao R, Lindstrom TM,Sokolove J, Low-grade inflammation as a key mediator of the pathogenesis of osteoarthritis, Nat. Rev. Rheumatol 12 (2016) 580–592. [PubMed: 27539668]

[20]. Scanzello CR, Plaas A, Crow MK, Innate immune system activation in osteoarthritis: is osteoarthritis a chronic wound? Curr. Opin. Rheumatol 20 (2008) 565–572. [PubMed: 18698179]

[21]. Liu-Bryan R, Synovium and the innate inflammatory network in osteoarthritis progression, Curr. Rheumatol. Rep 15 (2013) 323. [PubMed: 23516014]

[22]. Mahajan L, Gautam P, Dodagatta-Marri E, Madan T, Kishore U, Surfactant protein SP-D modulates activity of immune cells: proteomic profiling of its interaction with eosinophilic cells, Expert Rev. Proteomics 11 (2014) 355–369. [PubMed: 24697551]

[23]. Wu X, Zhao G, Lin J, Jiang N, Li C, Hu L, Peng X, Xu Q, Wang Q, Li H,Zhang Y, The production mechanism and immunosuppression effect of pulmonary surfactant protein D via toll like receptor 4 signaling pathway in human corneal epithelial cells during Aspergillus fumigatus infection, Int. Immunopharmacol 29 (2015) 433–439. [PubMed: 26507163]

[24]. Liu Y, Zhu H, Yan X, Gu H, Gu Z, Liu F, Endoplasmic reticulum stress participates in the progress of senescence and apoptosis of osteoarthritis chondrocytes, Biochem. Biophys. Res. Commun 491 (2017) 368–373. [PubMed: 28728848]

[25]. Gardai SJ, Xiao YQ, Dickinson M, Nick JA, Voelker DR, Greene KE, Henson PM, By binding SIRPalpha or calreticulin/CD91, lung collectins act as dual function surveillance molecules to suppress or enhance inflammation, Cell 115 (2003) 13–23. [PubMed: 14531999]

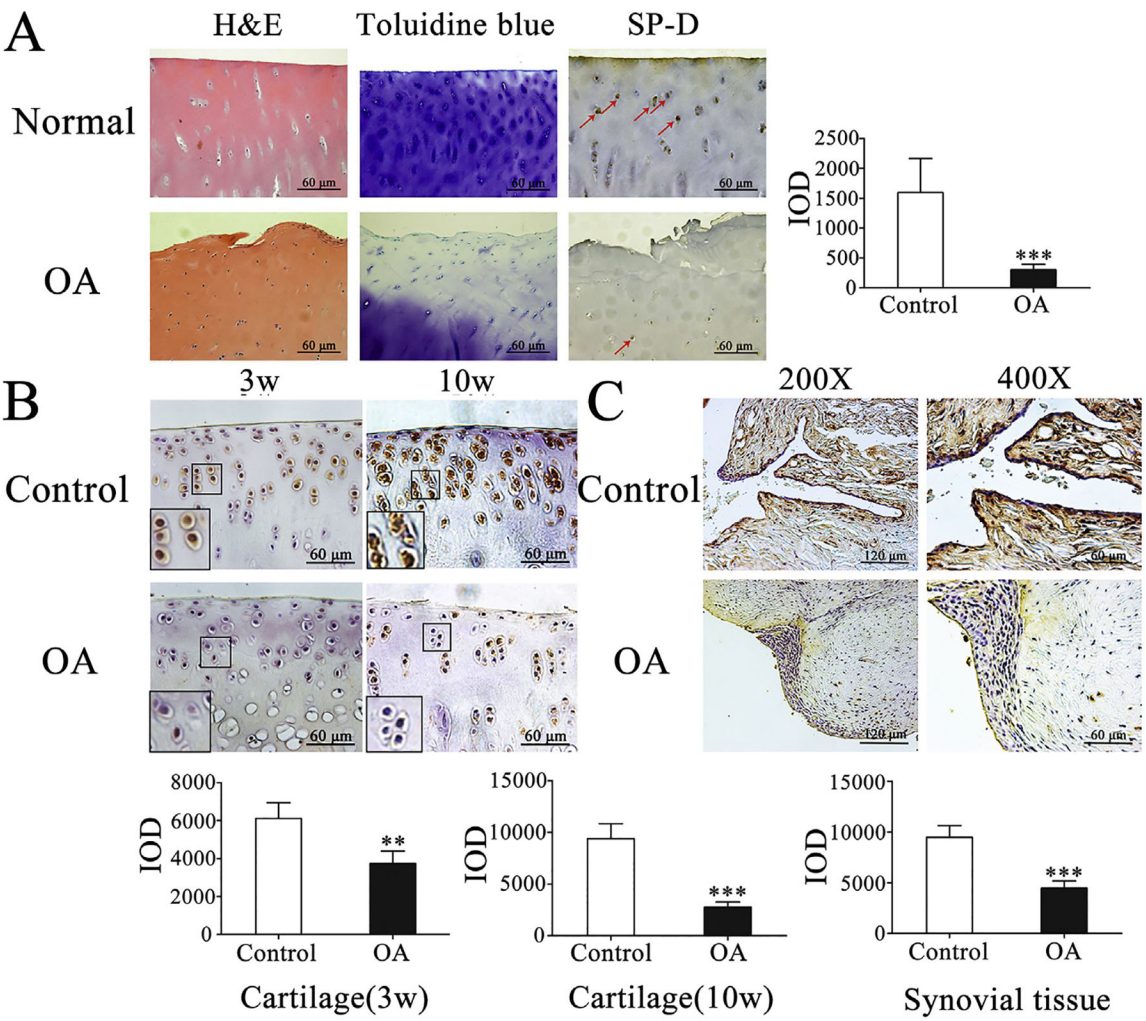

Fig. 1.

Expression of SP-D in human and rat articular cartilage by immunohistochemistry. (A) H&E and toluidine blue-O staining were performed and the expression of SP-D was detected in human normal and OA cartilage. Positive staining of SP-D pointed by a red arrow was higher in human normal cartilage than in OA cartilage (n = 3). (B) The rat cartilage SP-D expression was considerably higher in control group than that of the third and tenth week OA-induction groups, respectively (n = 5). (C) The SP-D expression of synovial tissue was higher in control group than that of the tenth week OA-induction group (n = 5). IOD was obtained from five representative sections of each joint in randomly selected high power field (× 400 magnification). Each column represents mean ± S.E.M. **p < 0.01 and ***p < 0.001 versus the control group of human and rat joint tissues. (For interpretation of the references to colour in this figure legend, the reader is referred to the web version of this article.)

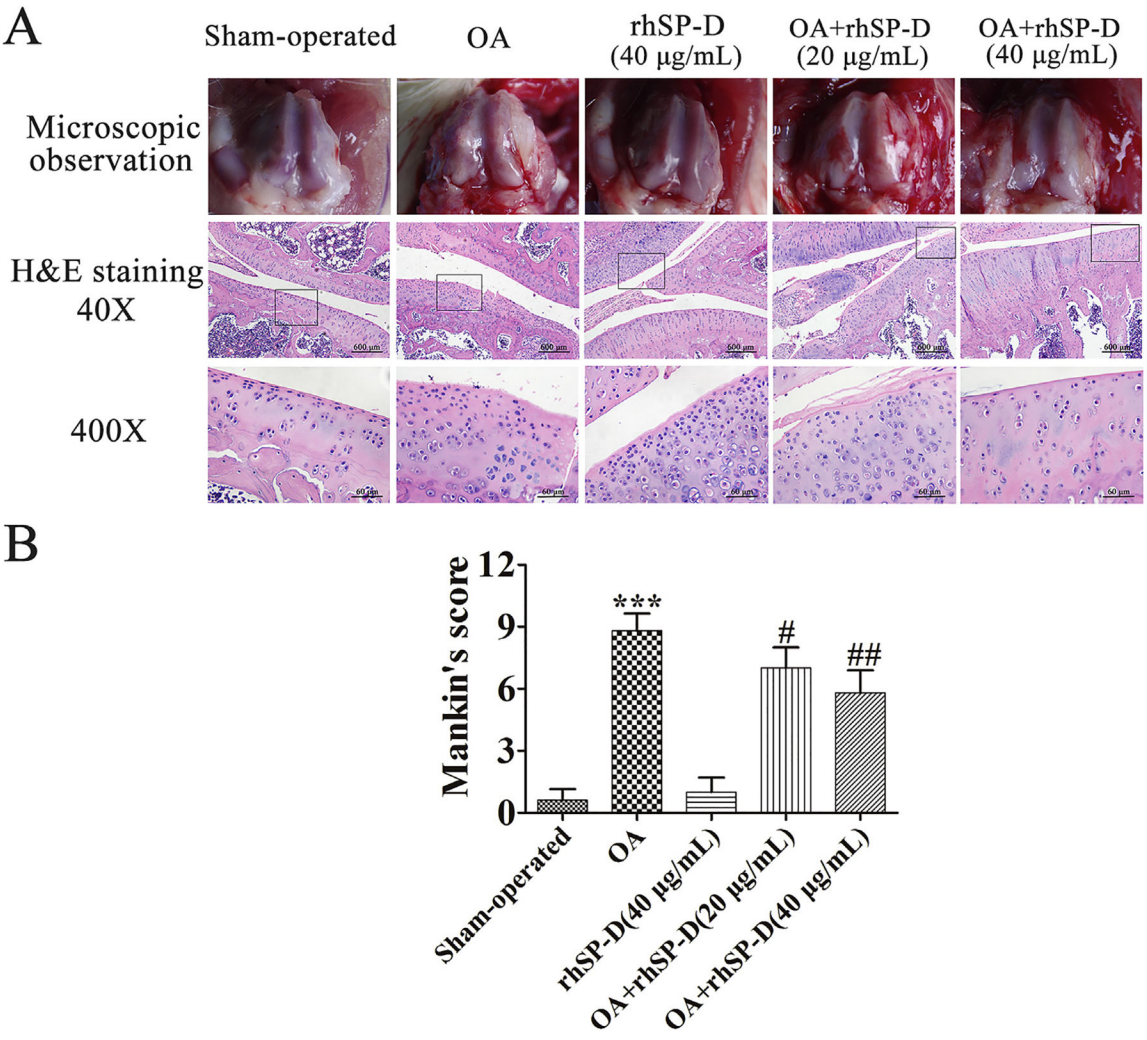

Fig. 2.

rhSP-D ameliorated cartilage degeneration in surgically-induced rat OA model. (A) Gross morphology, histological analyses of rat articular cartilage by H&E staining in each group. Magnification = × 40 (upper), × 400 (lower). (B) Histopathological scores were performed by the modified Mankin scores. Each column represents mean ± S.E.M (n = 5) ***$p < 0.001$ versus the sham-operated group; $^{\#}p < 0.05$ and $^{\#\#}p < 0.01$ versus the OA-induction group.

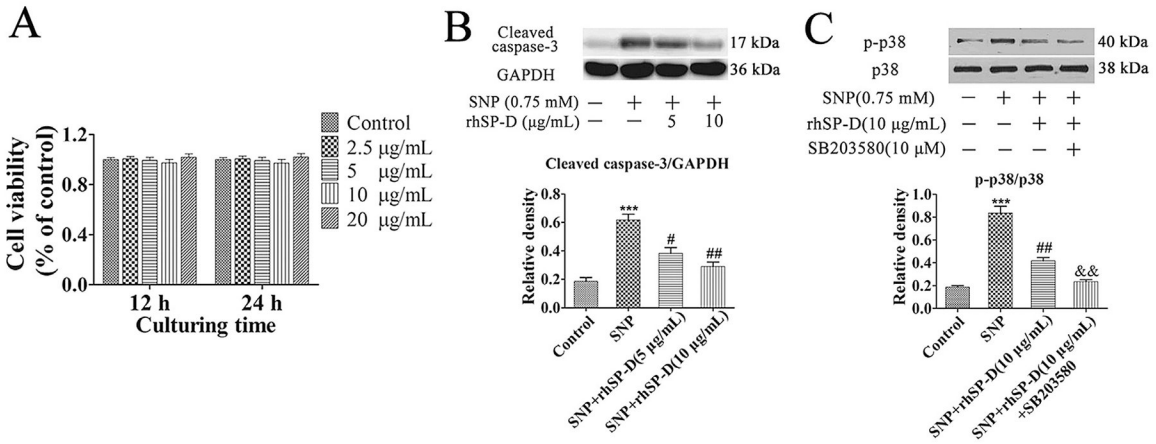

Fig. 3.

Cell viability and p38 MAPK signaling pathway is involved in the anti-apoptotic effect of rhSP-D on SNP-stimulated rat chondrocytes. (A) The rat chondrocytes were exposed to rhSP-D at concentrations ranging from 5 to 20 μg/mL for 12 and 24 h. (B–C) Chondrocytes were pre-treated with different concentrations of rhSP-D (5 and 10 μg/mL) in the presence and absence of the p38 MAPK inhibitor SB203580 (10 μM) for 2 h before 0.75 mM SNP co-treatment for 24 h. The protein levels of cleaved caspase-3, p-p38 MAPK and p38 MAPK were determined by Western blot. GAPDH was used as the internal control. Each column represents mean ± S.E.M (n = 3). ***$p < 0.001$ versus the control group; $^{\#}p < 0.05$ and $^{\#\#}p < 0.01$ versus the SNP group; $^{\&\&}p < 0.01$ versus the SNP + rhSP-D (10 μg/mL) group.

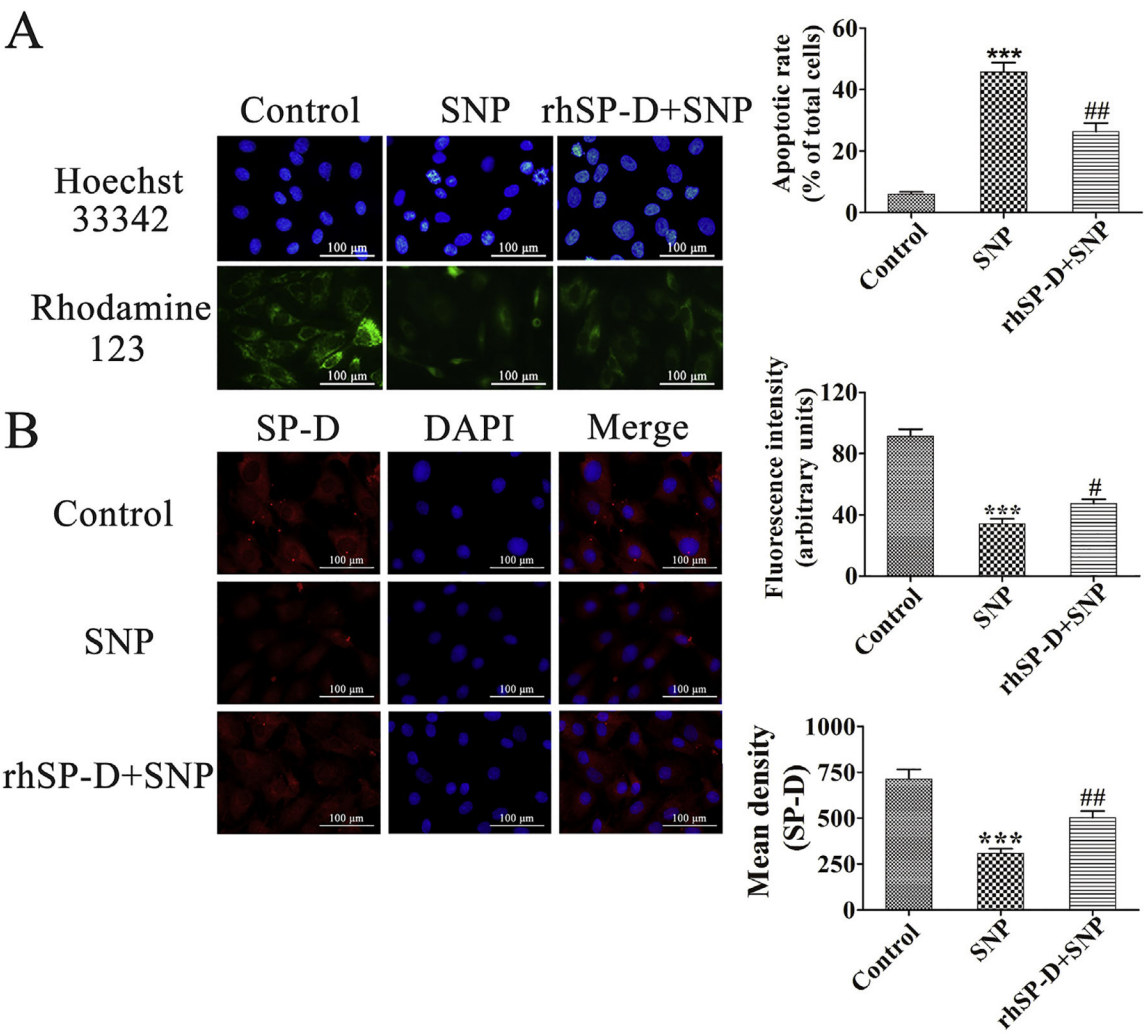

Fig. 4.

Effect of rhSP-D on the nuclear morphology, mitochondrial membrane potential, and SP-D expression of SNP-stimulated chondrocytes. (A) Hoechst 33342 staining and Rhodamine-123 staining of chondrocytes exposed to 10 μg/mL rhSP-D for 2 h before 0.75 mM SNP co-treatment for 24 h. The levels of chondrocyte nucleic morphologic changes and intracellular Rhodamine-123 fluorescence were evaluated. (B) Fluorescent images with SP-D-trakcer red of chondrocytes pre-incubated with 10 μg/mL rhSP-D for 2 h before 0.75 mM SNP co-treatment for 24 h. The apoptotic rate and mean density of fluorescence in each group were calculated. Each column represents mean ± S.E.M (n = 5). ***$p < 0.001$ versus the control group; $^{\#}p < 0.05$ and $^{\#\#}p < 0.01$ versus the SNP group. (For interpretation of the references to colour in this figure legend, the reader is referred to the web version of this article.)